International Conference on the Physics of Reactors "Nuclear Power: A Sustainable Resource"
Casino-Kursaal Conference Center, Interlaken, Switzerland, September 14-19, 2008

Developments within WIMS10

Tim Newton[a]*, Glynn Hosking[a], Les Hutton[a], David Powney[a], Brian Turland[a] and Ted Shuttleworth[a]

[a] *Serco, Dorchester, UK*

Abstract

The WIMS code provides a versatile software package for neutronic calculations, which can be applied to all thermal reactor types including mixed moderator systems. It can provide lattice cell and supercell calculations to produce the neutronic libraries for use in PANTHER or other whole core analysis codes; it can also be used for a complete analysis of small reactors.

WIMS provides a range of flux solution methods, including diffusion, S-n, collision probability and the method of characteristics. It can also use the MONK Monte Carlo solver and includes a hybrid perturbation solution method, MAX. WIMS allows the user to assemble a calculational route using these solvers, and a set of cross-section self-shielding methods and utility routines for data transfers and manipulation (e.g. condensation). Key data are stored on WIMS interfaces that are updated by the various processes.

Development of the WIMS code has continued to extend its capabilities and its range of application. The WIMS9 code was released in 2004, which included an improved treatment of resonance self-shielding, both using equivalence and sub-group methods. The latest version of the code, WIMS10, will be released in 2008.

1. Recent Developments of the WIMS code

The major advances in WIMS10 are:

- the development of a 3-D transport solver for flexible geometry using the Method of Characteristics;
- the extension of the sub-group method to allow for temperature variations in the fuel, and the ability to calculate a self-consistent fuel temperature profile;
- perturbation models for collision probabilities and diffusion;
- the incorporation of ECCO to provide greater resolution of the high energy spectrum and extend analyses to fast as well as thermal reactor systems;
- JEFF3 based nuclear data library;
- inclusion of full nuclide and material dependence in the fission spectra;
- improved input features including the use of parameters and equations in input data and the use of nested cycles;
- introduction of graphical outputs for checking model geometries and plotting results.

The first two of these developments are described below. Work is underway for future releases of WIMS as described in Section 4.

2. Three-dimensional Method of Characteristics

The Method of Characteristics, as implemented in the CACTUS module, has been in use in the

WIMS code for more than 20 years. The implementation allowed the treatment of general 2-D geometries for a Cartesian or hexagonal lattice (or super-cell) arrangement. In CACTUS a set of lines are constructed which by, reflection or translation at the lattice boundaries, return to their starting points within the model. The neutron transport equation is integrated along these lines to enable angular and scalar fluxes to be calculated.

The extension from 2-D geometry to a full 3-D geometry requires that lines are now explicitly traced along a 3-D path. Once the line lengths, and the interception points of lines with internal model boundaries, have been calculated, much of the existing framework of the CACTUS flux solver can be used.

The 3-D version of CACTUS uses geometry specification in the form of that used by the MONK and MCBEND Monte Carlo codes. This powerful 3-D geometry package is called Fractal Geometry (FG). This modelling system comprises two complementary components:

- a solid body package, which combines easy-to-use hierarchical constructs with the full versatility of the combinatorial geometry (CG) approach
- a "hole" geometry employing Woodcock tracking.

The FG package is supported by a range of graphic codes for model display and validation.

A new module has been written to accept solid body FG input (which allows shapes such as boxes, spheres, rods, prisms, cones) and to generate the line data required by the 3-D version of CACTUS. At present, the "hole" geometry feature is not available within 3-D CACTUS.

This new module, which processes the FG input, allows CACTUS to model a general 3-D geometry; it can also be used to generate inputs for 2-D problems. Lattice and supercell models may be constructed. In principle, the method can be applied to whole reactor analysis by constructing a "lattice" of cells with suitable absorption external to any reflector region.

Figure 1: Illustration of AGR Assembly Model used for CACTUS-3D Validation Study. End-gap, grid and brace structural components are shown by variations in colour along the height of the model.

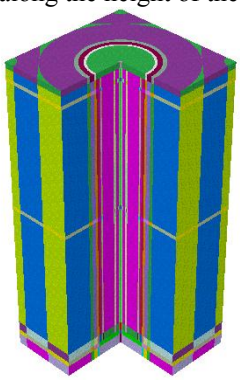

The use of the FG geometry package means that exactly the same base geometry input can be used for deterministic calculations with CACTUS-3D and Monte Carlo calculations with MONK. This provides an ideal means of assessing the effects of simplifications in the production of deterministic routes.

Test calculations of CACTUS-3D have included modelling a homogeneous cube with reflective boundary conditions on its ±y and ±z faces and a free boundary condition on its ±x faces. The model was solved in 69 energy groups. The CACTUS-3D k-effective was compared with that from a benchmark MONK calculation using the same cross-sections as CACTUS-3D. The difference between the codes' k-effective predictions was 70 ± 20 pcm. This indicates that CACTUS-3D can provide good reactivity estimates for simple models with 3-D, asymmetric flux profiles.

Validation calculations have also been made for more-complex 3-D geometries. One such case considered a model representing the principal 3-D geometric features of an un-poisoned AGR fuel assembly, solved in 2 energy groups. This model included representations of the grid and brace

Table 1: Comparison of MONK and CACTUS-3D Thermal Flux Ratios for an AGR Assembly Model.

MONK Results	Inner Ring Fuel	Middle Ring Fuel	Outer Ring Fuel
Bottom/Centre Flux Ratio	1.29 ± 0.04	1.29 ± 0.03	1.17 ± 0.02
Top/Centre Flux Ratio	1.36 ± 0.04	1.32 ± 0.03	1.23 ± 0.03
CACTUS-3D Results	Inner Ring Fuel	Middle Ring Fuel	Outer Ring Fuel
Bottom/Centre Flux Ratio	1.26	1.25	1.16
Top/Centre Flux Ratio	1.27	1.28	1.20

Figure 2: Illustration of Advanced CANDU® Reactor geometry. The fuel bundles are horizontal while the reactivity control device is inserted into a vertical guide tube situated in the heavy water moderator.

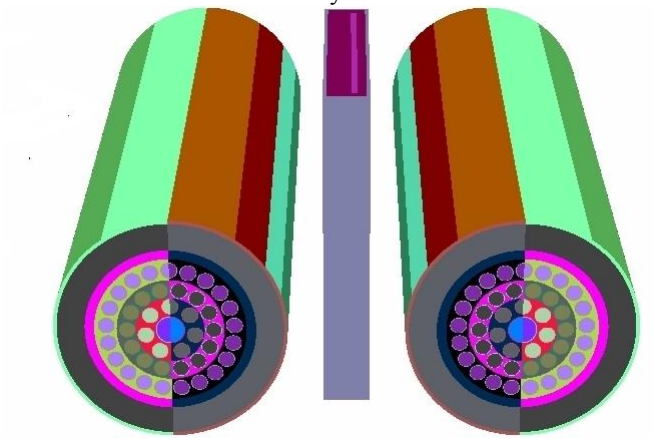

structural components, as well as the assembly end-gaps.

Figure 1 shows an illustration of the model. The CACTUS-3D predictions of k-infinity and fluxes were compared with those from a benchmark MONK calculation using the same cross-sections as CACTUS-3D. The difference between the codes' k-effective predictions was 167 ± 50 pcm. An important quantity from AGR calculations is the estimate of thermal flux peaking at the ends of an assembly. Table 1 shows the end/centre thermal flux ratios calculated by MONK and CACTUS-3D for each of the three rings of fuel pins. There is good agreement between the flux ratios predicted by the codes.

CACTUS-3D has also been applied to the assessment of the worth of reactivity control devices (RCDs) for an Advanced CANDU® type reactor.

The RCD that was modelled consists of a vertical guide tube in the moderator, which passes between pairs of horizontal fuel bundles. A steel plate is moved within the guide tube to provide reactivity control.

In line with current AECL practice, the requirement was to generate few-group incremental cross-sections due to (i) the presence of the guide tube alone and (ii) the full insertion of the steel plate (referred to as a control rod below) within the guide tube. This is a challenge for lattice codes as the geometry is fully 3-dimensional, thus there is a requirement to provide a fully three-dimensional model. Here, a 3-D lattice cell consists of two horizontal fuel bundles, with a vertical guide tube in which a control rod may be inserted.

CACTUS-3D uses the geometry package of the Monte Carlo code MONK. It is therefore straightforward to run benchmark Monte Carlo calculations in the same geometry for model verification purposes. This capability was used to provide confidence in the CACTUS-3D calculations. (Note that as CACTUS-3D is a deterministic code, it is much simpler to extract the difference of two cross-sections than is the case for a Monte Carlo code with stochastic uncertainties.)

Figure 2 shows the basic cell geometry that is modelled. The cell consists of two fuel bundles with surrounding moderator. The depth of the cell is the length of one fuel bundle (~0.50 m); the lattice pitch is 0.24 m. The guide tube is located in the moderator. The same geometry was used for the generation of incremental cross-sections for the RCD components as used previously with the DRAGON code, which is used by AECL for the generation of the incremental cross-sections. As there are slight asymmetries in the positioning of the guide tube and control rod, it is necessary to consider two fuel bundles associated with the RCD, giving total dimensions for the "lattice" cell of 0.5 m x 0.24 m x 0.24 m. Reflective boundary conditions are assumed on all faces of this cell.

Three calculations are performed:

1. With neither the guide tube nor the control rod present (both replaced by moderator in the model).
2. With the guide tube present and the control rod absent (replaced by moderator in the model).
3. With the guide tube present and the control rod fully inserted.

It is required to determine the changes in the two-group cross-sections (absorption, fission, nu-fission, scatter) and the two-group diffusion coefficients as 1→ 2 and 2→ 3 above (i.e. as first the guide tube is inserted, and secondly the control rod is inserted) for a region consisting of the two half fuel-bundles (and associated coolant, moderator and structures) facing the RCD.

There are four stages to the WIMS calculations:

1. Formation of the self-shielded cross-sections.
2. Generation of the condensation spectrum for the whole model and the calculation of broad group cross-sections using approximate geometry.
3. The CACTUS-3D solution using the broad group data in exact geometry.

® CANDU is a registered trademark of Atomic Energy of Canada Limited

4. Condensation of the cross-sections to two groups (with an energy partition at 0.625 eV), and the generation of incremental cross-sections for comparison with those obtained with DRAGON.

In these demonstration calculations the CACTUS-3D solution was obtained in 6 and 11 energy groups. These are standard energy partitions adjusted to be consistent with the required two group boundary. They have previously been found to provide sufficient energy resolution for such problems. However, it is anticipated that, if necessary, CACTUS-3D could reasonably use 20 – 30 groups.

In the WIMS model, the central pin and the three rings of pins are each represented as consisting of different materials, which will burn up differently during the calculation. The central pin of the fuel bundle contains dysprosium. The WIMS module HEAD is used to generate self-shielded cross-sections by the equivalence method. In addition there is a separate treatment of self-shielding for U^{235}, U^{238} and Dy^{163}. These use the sub-group method for the cluster geometry (fuel bundle and surrounding moderator). The sub-group solution is obtained using collision probabilities (the PIJ method which obtains collision probabilities by a tracking method). Initial calculations were performed for fresh fuel; in this case it is possible to generate the broad group cross-sections at this stage. However, the final specification required the use of fuel at mid burn-up. For this case, the spectrum within a single bundle and its associated moderator was calculated in 172 groups (the library structure) using collision probabilities for the two-dimensional fuel bundle model. This was used to derive the pin compositions at the specified burn-up, using critical bucklings, with re-shielded cross-sections calculated periodically (91 cycles were used to achieve the specified burn-up of 4843 MWd/tonne). The compositions and fluxes are stored on an interface for use in the 3-D model.

Figure 3: Two-dimensional vertical section through the fuel bundles and reactivity control device, showing the separation into different materials.

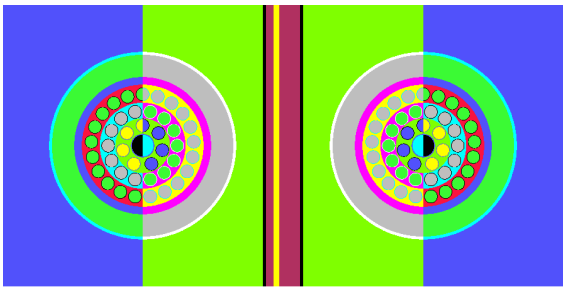

As discussed above the three-dimensional model is set up using the FG solid geometry package developed for MONK. Composition and flux data for the 172 groups are read from the interface and condensed to the broad-group (6 or 11 group) structure. In the case where the guide tube (and also the control rod) is present, this condensation uses an approximate method to couple the fuel bundles with the guide tube (and control rod structure); again collision probability methods are used to obtain the spectrum for the condensation.

As shown in Figure 3, at this stage of the calculation the pins within a ring are treated as different materials depending on whether or not they face the reactivity control device; this allows the code to distinguish the parts of the bundle and associated moderator that are to be condensed to obtain the final two-group sections.

The final calculation model used in the CACTUS-3D calculation (Figures 2 and 3) has a mesh of 0.5 cm cubes in the moderator, 4 azimuthal meshes in the cylindrical parts and a projected track separation of 0.04 cm, which is equal to the mesh dimension in the fuel clad. The polar axis of the model is aligned with the axis of the fuel bundles; the projected track separation is the separation projected on to a plane perpendicular to the fuel

.**Table 2:** Differences between the CACTUS-3D and MONK Results for Advanced CANDU Reactivity Control Device Model with Fresh Fuel.

No of groups used in MONK	6	11	172	172
No of groups used in CACTUS-3D	6	11	6	6
Control rod in (% difference in k-infinity)	0.37	-0.63	-1.12	-1.17
Control rod out (% difference in k-infinity)	0.02	-0.19	-0.52	-0.63
Control rod worth (% difference)	5.59	5.98	7.85	6.82

Figure 4: Schematic of the sub-group method for a resonance within a singe broad group. Note that the "weights" correspond to bands in the energy spectrum about the resonance peak.

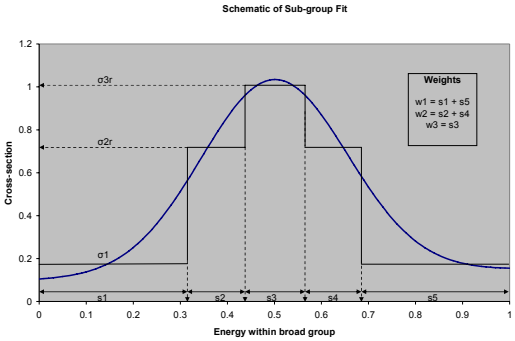

Figure 5: U238 Cross Section Ratio of Temperature Distribution to Profiled Temperature around the 36.7 Resonance

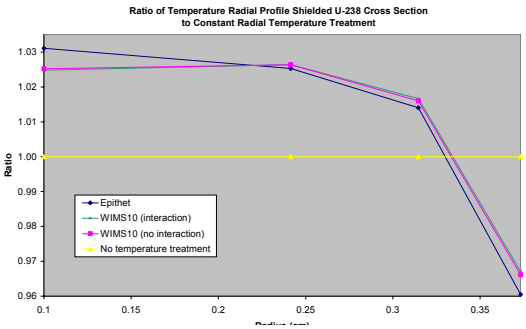

bundle. Eight separate polar and eight separate azimuthal angles were used; allowing for reflections from the boundaries, this corresponds to a total of 8 x 64 = 512 directions. It should be noted that not all tracks intersect all meshes (the sampling is of order 1 in 10); however there are sufficient tracks to obtain good estimates of the scalar flux for the neutron sources and sinks.

The CACTUS-3D model was verified by comparison calculations for fresh fuel with MONK; the MONK model used identical geometry. Differences in k-infinity for the cases with the control rod in and out are shown in Table 2. The MONK results indicate that in evaluating k-infinity there is a significant effect in the reduction from 172 groups (in MONK) to the number of groups (6 or 11) used in the CACTUS calculations. This effect is up to 800 pcm. This effect is greatest for the rod in calculation, but is still significant for the rod out case.

MONK (in broad groups, as used here) and CACTUS-3D use the same nuclear data library, although, it should be noted that MONK does not treat negative scatter cross-sections which can influence results in many groups. However, in these MONK calculations P1 scatter is modelled explicitly, while CACTUS-3D assumes P0 scattering, with cross-sections corrected for the P1 term. It is seen, from Table 2, that, for the rod out case, the differences arising from the lack of P1 scatter and the finite CACTUS meshing lead to differences of less than 200 pcm in k-infinity.

Table 3: Comparison of normalised incremental cross-sections calculated using DRAGON (supplied by AECL) and calculated using CACTUS-3D. Results are shown as percentages of the homogenised cross-sections for the fuel bundle only.

Control rod	DRAGON	CACTUS (6 groups)	CACTUS (11 groups)
Absorption – fast group	2.1	2.3	2.4
Absorption – thermal group	17.7	17.9	18.0
Nu-fission – fast group	-0.24	-0.31	-0.24
Nu-fission – thermal group	3.4	3.44	3.5
Radial diffusion – fast group	-1.4	-1.1	-1.1
Radial diffusion – thermal group	-0.81	-0.85	-0.83
Axial diffusion – fast group	-1.3	-1.1	-1.1
Axial diffusion – thermal group	-0.81	-0.85	-0.83
Downscatter: fast to thermal	16.7	13.8	14.1
Power – fast group	-0.23	-0.28	-0.22
Power – thermal group	3.4	3.4	3.4

However, when the control rod is inserted, these differences increase. This has an impact on the calculated worth of the control rod, where the sum of the condensation and the P1 effect lead to discrepancies of up to 8% in the control rod worth. This suggests that further optimisation of the meshing and condensation processes might be beneficial for the k-infinity values, along with a more detailed investigation of the importance of P1 scatter in this application. However, CACTUS-3D results were judged to be sufficiently encouraging to proceed with the analysis of the mid-burnup case.

CACTUS-3D results for the incremental cross-sections for the mid-burnup case are compared with values (supplied by AECL) obtained using the DRAGON code in Table 3. The incremental cross-sections are expressed as percentages of the CACTUS-3D homogenised data for a fuel assembly. The results show a broad agreement between the incremental cross-sections calculated with CACTUS-3D and the reference values supplied by AECL. In particular, the thermal absorption cross-section for the control rod is predicted to increase by ~17.9%, compared with the reference value of 17.7%.

Subsequently the route developed with CACTUS-3D has been implemented in a version of WIMSBUILDER developed for CANDU reactors allowing production calculations to be performed for different burn-ups and reactivity control device parameters.

3. Extension of the sub-group method for varying temperatures

The self-shielding due to resonances is considered in WIMS using either equivalence or sub-group methods. Both of these approaches use resonance integrals, evaluated with NJOY for a homogeneous system consisting of the nuclide in question and a background scatterer. The resonance integrals are tabulated as a function of temperature and the equivalent "hydrogen-like" scatter. The sub-group method requires the assignment of a set of cross-sections and accompanying "weights" (or "widths") to a particular resonance. Originally, a single set of cross-sections was used for all resonances of a particular nuclide. This involved a fit to the mean resonance integrals over the resonance range. With this set of cross-sections, the flux for each sub-group could be calculated using, for instance, collision probabilities or the method of characteristics. Only one flux calculation was then required for each sub-group. When individual resonances were considered, the resonance integrals, with various values of the scattering parameters, were used to derive appropriate weights for the individual resonance. Having solved for the fluxes and weights, it was then straight-forward to derive the self-shielded broad group cross-sections for the materials in the model.

The energy range for which resonances were considered was extended in WIMS9 to cover 4eV to 123keV. It was found that improved results could be obtained if each resonance was fitted individually (i.e. it had its own optimised set of cross-sections and weights consistent with the resonance integrals). Figure 4 slows a schematic of the fitting of three (for clarity) cross-sections $\sigma 1$, $\sigma 2$, and $\sigma 3$ and their respective weights to a resonance. With this approach, the flux solution must be obtained for each value of the cross-section.

When oxide fuel is used there is likely to be a significant variation of temperature across the fuel. Previously a mean fuel temperature had been used in the calculation of the broad energy group cross-sections. However, it is preferable that the resonance treatment should be based on the local temperature. This is now possible. The weights are first fitted for the fuel average temperature using the tabulated resonance integrals. The cross-sections are then fitted using these weights for the different fuel regions, using the resonance integrals appropriate to the local temperature and broad energy group. Consideration of Figure 4 shows that this is the appropriate approach as the weights define local energy bands about the resonance peak. The method has considerable geometric flexibility and may be applied to any situation that can be modelled by collision probabilities or the method of characteristics.

WIMS now includes a module that allows the temperature profile in a pin to be calculated from the fission source, the fuel and clad thermal properties and the coolant boundary conditions. Temperature information has been added to the WIMS interface. This allows an iteration to be performed between the broad group cross-section calculation and the temperature field. Example results for a PWR pin show that the difference between the single set of sub-groups and the multi-sub group method only leads to a difference of 3 pcm in k-effective, when the average (Reichel) temperature is used; the use of multi sub-groups and multi temperatures leads to a

Figure 6: AGR Radial Geometry

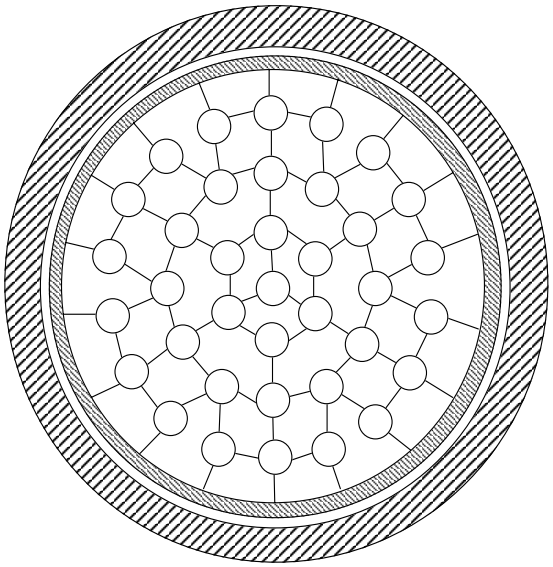

Figure 7: AGR Axial Geometry

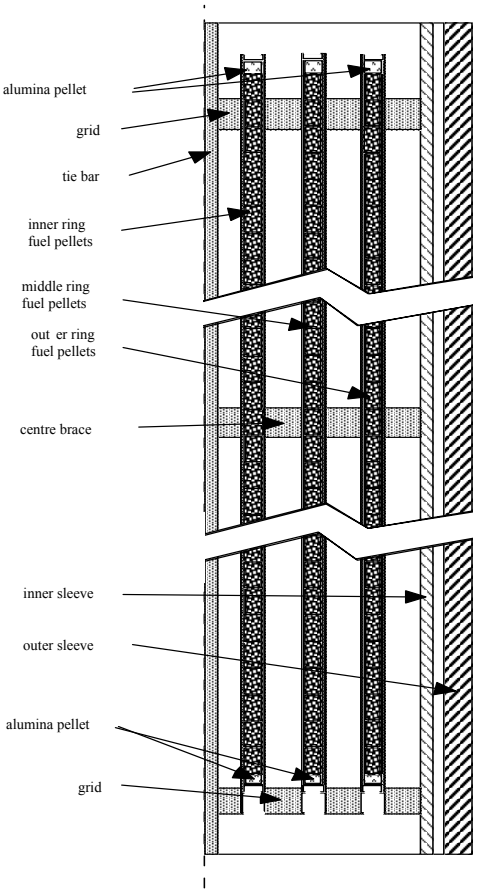

difference of 108 pcm. This approach will provide a reference method for depletion calculations

The method has been validated against the EPITHET code. EPITHET solves the slowing down equations in annular geometry using a detailed energy representation and therefore can be regarded as a reference solution. A typical PWR pincell at start of life, comprising fuel, cladding and moderator was taken as a test case. The fuel region was divided into 4 calculational meshes of equal area and was modelled with a temperature distribution representative of an operating PWR, and also with a uniform temperature derived by a volume weighted average. Shielded cross sections were derived by both WIMS10 and EPITHET for U^{238} in the energy range 26.61- 48.25 eV which spans the 36.7 eV resonance. The WIMS10 calculations employed the method of characteristics to calculate the subgroup fluxes based on a fixed slowing down source. The ratio of the cross sections for the temperature distribution to those for the uniform temperature is given in Figure 5. Within WIMS10 there are two approaches to modelling the interaction between resonance isotopes. At higher energies where the resonances are closer in energy a random interaction is assumed; at the lower energies, such as we are considering here, where the resonances are distinct, the interaction is based on factors calculated from an auxiliary slowing down calculation. The WIMS10 calculations were performed with this interaction between U^{235}, and with U^{238} modelled and also for U^{238} alone.

With reference to Figure 5 it can be seen that modelling a temperature profile changes the shielded cross section by around -4% at the edge of the pin and around +3% at the centre of the pin. The effect is well predicted by the model in WIMS10. Further scoping calculations indicate that this improved modelling technique will only have a small effect on k-infinity but may reduce doppler coefficients ($d\rho/dT$) by around 6%.

4. Future Development

Work is underway to develop WIMS further, including greater whole-core capabilities. CACTUS-3D will be extended to use MONK's "hole" geometry for input. The longer term goal is to ensure the robustness and efficiency of the

Figure 8: AGR Cluster Axial Power Distributions calculated by MONK and MAX

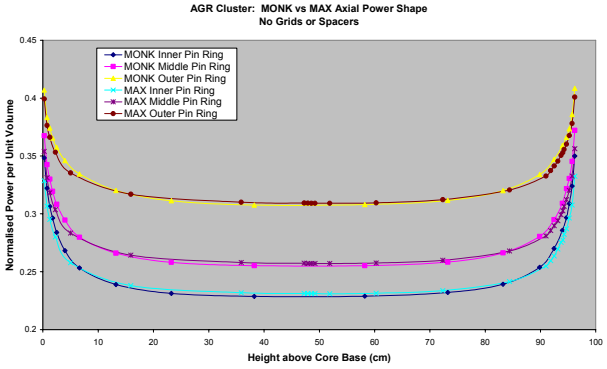

Figure 9: AGR Cluster Axial Power Distribution with Steel Grids and Braces included

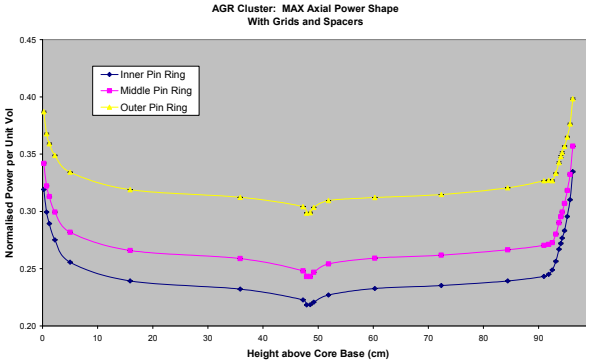

method of characteristics for larger problems. Currently the acceleration methods used in CACTUS are optimised for lattice cell applications; whole core applications pose different challenges, in particular in the reflector region. Investigations are underway to examine the effectiveness of using a coarse-mesh, diffusion-like solution to accelerate the convergence of a detailed CACTUS calculation. Other developments aim to optimise the line configuration, so that good spatial coverage is obtained with as few lines as possible. For whole-core calculations, line optimisation using a "once-through" approach is being considered. Here, lines pass directly from one side of a model to the other and are not reflected or translated off model boundaries. A benefit of this approach is that it is relatively straightforward to ensure uniform line coverage.

WIMS includes a module, MAX, which solves the exact perturbation equations using a Monte Carlo approach. MAX requires a base solution for the flux and the adjoint flux from a transport module, such as CACTUS. Previously MAX has been used to extend a 2-D solution into a 3-D solution, by introducing the difference between the 2-D and 3-D geometries as a perturbation. The method is particularly effective in the estimation of reactivity coefficients, as convergence is determined by the size of the perturbation, rather than the underlying base solution. This makes this hybrid approach a cost-effective means in production calculations. Because MAX uses a Monte Carlo approach to score the perturbations, it is now being incorporated into the MONK code. This will allow a common geometry input with MONK and CACTUS-3D. Estimating the uncertainty on calculated results is becoming increasingly important in many applications. Currently some perturbation methods are available to estimate sensitivity to some parameters. Work will continue to extend the range of sensitivity/uncertainty tools available including the use of covariance data.

The MAX module of WIMS has been validated against MONK for fuel assemblies of the British Advanced Gas-cooled Reactor (AGR) design. The AGR see Figures 6 and 7 contains cluster fuel assemblies which are moderated by graphite and cooled by carbon dioxide. The fuel pins comprise pellets of enriched uranium dioxide enclosed in a stainless steel tube. The pins are arranged in three rings with 6, 12, and 18 pins in the first, second, and third ring respectively. Axial power distributions for this type of assembly, calculated by MAX and MONK are given in Figure 8 . It can be noted that the reference result is well predicted by MAX. MAX can also be used to calculate a more detailed axial solution. See Figure 9 for example where the steel braces, used to locate the fuel pins, are included in the model.

Developments will continue to enhance the code user image and graphical display of output. The aim is to reduce the time required to perform and understand the results of a calculation by simplifying the input and optimising the graphical display of the vast amounts of data generated.

5. Acknowledgements

The CACTUS-3D model for the reactivity control device was developed and run by Yevgen Kudelin. The authors thank AECL for their support for this work, the technical input of Julian Lebenhaft and Tahar Sissaoui, and for permission to publish.